Published in final edited form as:
*Bioorg Med Chem*. 2009 July 1; 17(13): 4797–4805. doi:10.1016/j.bmc.2009.04.034.

# A Versatile Photoactivatable Probe Designed to Label the Diphosphate Binding Site of Farnesyl Diphosphate Utilizing Enzymes

**Olivier Henry**[a], **Fernando Lopez-Gallego**[b], **Sean A. Agger**[b], **Claudia Schmidt-Dannert**[b], **Stephanie Sen**[c], **David Shintani**[d], **Katrina Cornish**[e], and **Mark D. Distefano**[a,*]

[a]Department of Chemistry, University of Minnesota, 207 Pleasant Street SE, Minneapolis, MN 55455

[b]Department of Biochemistry, Molecular Biology and Biophysics, University of Minnesota, 1479 Gortner Avenue, St. Paul, MN 55108

[c]Department of Chemistry, The College of New Jersey, P.O. Box 7718, Ewing, NJ 08628

[d]Department of Biochemistry, University of Nevada, Reno, NV 89557

[e]Yulex Corporation, 37860 W. Smith-Enke Road, Maricopa, AZ 85238

## Abstract

Farnesyl diphosphate (FPP) is a substrate for a diverse number of enzymes found in nature. Photoactive analogues of isoprenoid diphosphates containing either benzophenone, diazotrifluropropionate or azide groups have been useful for studying both the enzymes that synthesize FPP as well as those that employ FPP as a substrate. Here we describe the synthesis and properties of a new class of FPP analogues that links an unmodified farnesyl group to a diphosphate mimic containing a photoactive benzophenone moiety; thus, importantly, these compounds are photoactive FPP analogues that contain no modifications of the isoprenoid portion of the molecule that may interfere with substrate binding in the active site of an FPP utilizing enzyme. Two isomeric compounds containing *meta*- and *para*-substituted benzophenones were prepared. These two analogues inhibit *S. cerevisiae* protein farnesyltransferase (ScPFTase) with $IC_{50}$ values of 5.8 (*meta* isomer) and 3.0 μ*M* (*para* isomer); the more potent analogue, the *para* isomer, was shown to be a competitive inhibitor of ScPFTase with respect to FPP with a $K_I$ of 0.46 $\mu$M. Radiolabeled forms of both analogues selectively labelled the β-subunit of ScPFTase. The *para* isomer was also shown to label *E. coli* farnesyl diphosphate synthase and *Drosophila melanogaster* farnesyl diphosphate synthase. Finally, the *para* isomer was shown to be an alternative substrate for a sesquiterpene synthase from *Nostoc sp. strain PCC7120*, a cyanobacterial source; the compound also labeled the purified enzyme upon photolysis. Taken together, these results using a number of enzymes



*Corresponding author. Tel.: 612-624-0544; fax: 612-626-7541. E-mail address: diste001@umn.edu.



**Supplementary Data**

$^{1}$H NMR spectra for **6a, 7a, 7b, 8a, 8b, 4a** and **4b**, $^{31}$P NMR spectra for **6a, 7a, 7b, 8a, 8b, 4a** and **4b**, HR-ESI-MS spectra for **4a** and **4b** and HPLC chromatograms for **4a** and **4b** are included. Stereo images of the models shown in Figure 8 are included along with several tables that summarize important distances within the active site of each enzyme model. Pymol files for each of the enzyme models are also provided.

demonstrate that this new class of probes should be useful for a plethora of studies of FPP-utilizing enzymes.

**Keywords**

Benzophenone; Farnesyl Transferase; Farnesyl Diphosphate Synthase; Sesquiterpene Cyclase; Photoaffinity Labeling

## 1. Introduction

Farnesyl diphosphate (FPP, **1**) is a substrate for a large number of enzymes found in nature. The products of such enzymes include sesquiterpene natural products,[1, 2] side-chains of cofactors,[3] biopolymers such as latex[4] and lipidated proteins.[5] Given the vast number of natural products derived from FPP and the medicinally important properties of many of them, the development of new probes that can be used to identify FPP-utilizing enzymes is an important area of inquiry.[6] Photoactive analogues of isoprenoid diphosphates containing either benzophenone,[7–16] diazotrifluropropionate[17–23] or azide[24, 25] groups have been useful for studying both the enzymes that synthesize FPP as well as those that employ FPP as a substrate such protein prenyltransferases. To date, most photoaffinity labeling analogues of FPP (see Figure 1, 2 and 3) incorporate the light-absorbing functionality into the isoprenoid moiety itself. While such molecules have proved to be useful, they are limited by the fact that they are only capable of labeling residues located within the isoprenoid binding site. Moreover, in cases where the overall size and shape of the active site is highly constrained, probes that incorporate bulky modifications in the prenyl group may not effectively bind. Those limitations led us to design a new type of FPP analogue (**4a** and **4b**) that would incorporate an unmodified farnesyl group linked to a diphosphate mimic containing a photoactive benzophenone moiety. Here we describe the syntheses of these two analogues and evaluate their ability to bind and label several different FPP utilizing enzymes.

## 2. Results

### 2.1. Synthesis of farnesyl diphosphate analogue incorporating a benzophenone photophore into the diphosphate group

The isomeric photoactive analogues **4a** and **4b** were prepared using the route summarized in Scheme 1. For the preparation of the *meta* isomer **4a**, commercially available 3-methyl-benzophenone **5a** was brominated in presence of NBS in $CCl_4$ at reflux to yield the 3-bromo-methyl-benzophenone (**6a**). The crude material was then treated in neat trimethylphosphite at reflux to produce the desired diester **7a** in good yield (85% from **5a**) followed by hydrolysis under acidic conditions to afford the unprotected phosphonate **8a** in 49% yield. Coupling of **8a** to farnesyl monophosphate (**9**) was achieved through the reaction of the two components with carbonyldiimidazole in DMF and the purified product (**4a**) was obtained in 15% yield after ion exchange chromatography followed by reversed-phase chromatography. Compound **4a** was characterized by $^{1}$H-NMR, $^{31}$P-NMR, HR-ESI-MS and UV spectroscopy. The isomeric probe **4b** was obtained from an analogous route beginning with commercially available 4-bromo-methyl-benzophenone (**6b**). For the photoaffinity labeling experiments described below, it was necessary to prepare **4a** and **4b** in radiolabeled form. In earlier work, we developed a simple method for the preparation of $^{32}$P-labeled FPP and related analogues;[26, 27] a variation of that method was employed here, shown in Scheme 2, to obtain the desired labeled probes.

First, farnesyl monophosphate ([$^{32}$P]**9**) was synthesized through the reaction of farnesol (**10**) with [$^{32}$P]$H_3PO_4$ using $CCl_3CN$ as the coupling agent. The radiolabeled product ([$^{32}$P]**9**)was

purified using a disposable Sep-Pak reversed-phase column and then coupled with **8a** or **8b** in the presence of CDI in DMF to yield **4a** or **4b**, respectively. The radiolabeled probes were again purified using a disposable Sep-Pak reversed-phase column and their radiochemical purities (> 80%) were assessed by TLC followed by phosphorimaging analysis.

### 2.2. Enzymatic studies with protein farnesyltransferase using 4a and 4b

The utility of the new probes were first evaluated in experiments with purified *S. cerevisiae* protein farnesyltransferase (ScPFTase) since that enzyme has been extensively characterized via structural and enzymological studies.[28–32] Importantly, its substrate specificity has been thoroughly investigated including a large number of isoprenoid diphosphate analogs that have been examined as inhibitors and alternative substrates.[10,11,15,17,33–38]

Compounds **4a** and **4b** were first analyzed as substrates for ScPFTase using a continuous fluorescence assay employing the pentapeptide *N*-dansyl-GCVIA as the prenyl group acceptor. This assay monitors the increase in fluorescence of the dansyl group upon prenylation at the neighboring cysteine residue caused by the change in hydrophobicity as previously described.[39,40] No observable change in the fluorescence of the pentapeptide was observed in reactions containing **4a** or **4b** in place of FPP at concentrations up to 200 μM, which suggests that these molecules are not substrates for ScPFTase.

To evaluate their potential as enzyme inhibitors, the rate of ScPFTase-catalyzed farnesylation of Ds-GCVIA was measured at a fixed concentration of FPP and varying concentrations of **4a** and **4b**. In those reactions, the presence of **4a** or **4b** attenuated the rate of peptide prenylation, indicating that these compounds are enzyme inhibitors. Plots of enzymatic rate versus concentration of inhibitor gave $IC_{50}$ values (Tabulated in Table 1) of 5.8 μM for **4a** and 3.0 μM for **4b**. To gain additional understanding of the mechanism of ScPFTase inhibition by these compounds, the more potent inhibitor, **4b**, was studied in greater detail. The rate of ScPFTase-catalyzed prenylation of Ds-GCVIA was measured in the presence of fixed concentrations of the isoprenoid substrate, FPP, and varying concentrations of **4b**. Double reciprocal plots of those data gave a pattern of lines that intersect on the 1/V axis, consistent with competitive inhibition with respect to the substrate FPP (See Figure 2); this result is consistent with FPP and **4b** binding at the same site. Further analysis by the method of Eadie-Hofstee gave $K_I$ value of 0.48 μM for ScPFTase.[41,42]

We next evaluated $^{32}$P-labelled forms of **4a** and **4b** for their ability to label ScPFTase upon photolysis. In those experiments, each analogue was photolyzed in the presence of purified ScPFTase and the resulting reaction mixture was then fractionated by SDS PAGE. The total protein present was visualized by staining with Coomassie Blue and the labeled protein was detected via phosphorimaging analysis. Representative photolabelling results using [$^{32}$P]**4b** are shown in Figure 3. Photolysis of ScPFTase with [$^{32}$P]**4b** led to strong labeling of the β-subunit of the enzyme with minimal labeling of the α-subunit (Figure 3, Lane 2). The labeling was almost completely abolished when the photolysis was performed in the presence of both [$^{32}$P]**4b** and excess FPP (competition experiment, Figure 3, Lane 3); no labeling occurred in the absence of irradiation (Figure 3, Lane 1). Similar results were obtained in experiments with [$^{32}$P]**4a** (Data not shown).

### 2.3. Labeling studies of farnesyl diphosphate synthases (FPPSase) using 4b

As noted above, a number of studies have reported the successful labeling of protein prenyltransferases using photoactive analogues. In contrast, there are relatively few reports of such probes being used to label FPPSases involved in the biosynthesis of isoprenoids. Accordingly, we examined the ability of **4b** to label FPPSases from two different sources. First [$^{32}$P]**4b** was photolyzed in the presence of *E. coli* FPPSase IspA (EcFPPSase)[43] under

conditions similar to those used for PFTase described above; results from those experiments are shown in Figure 4. Photolysis of EcFPPSase with [$^{32}$P]**4b** led to strong labeling of the purified enzyme (Figure 4, Lane 2) which was substantially (although not completely) reduced when the photolysis was performed in the presence of both [$^{32}$P]**4b** and FPP (competition experiment, Figure 4, Lane 3); no labeling occurred in the absence of irradiation (Figure 4, Lane 1).

To further examine the utility of probe **4b**, labeling experiments were carried out using DmFPPSase,[44] an insect-derived enzyme from *Drosophila melanogaster*. Photolysis of purified DmFPPSase with [$^{32}$P]**4b** resulted in labeling of the enzyme (Figure 5, Lane 1); no labeling was observed without irradiation (Data not shown). When photolysis was performed in the presence of both [$^{32}$P]**4b** and FPP as a competitor (Figure 5, Lane 2), a significant decrease (46% of the labeling obtained in the absence of the competitor) in the amount of labeling was observed.

### 2.4. Experiments using 4b with a sesquiterpene synthase

Another major class of important FPP-utilizing enzymes is the sesquiterpene synthases. To evaluate the utility of the diphosphate-directed photoprobes developed here to interact with this class of enzymes, experiments were performed using a sesquiterpene synthase from *Nostoc sp. strain PCC7120*, (NoSTSase);[45] that particular enzyme produces germacrene A from the cyclization of FPP. Initially, it was assumed that the phosphonophosphate functionality present in **4b** would not be processed by NoSTSase (as was the case with ScPFTase) and that the compound would hence serve as an inhibitor. Interestingly, addition of **4b** to reactions containing purified NoSTSase and FPP did not result in a decrease in the cyclized product indicating that **4b** was not an inhibitor of the enzyme. Instead, incubation of NoSTSase and **4b** alone (without FPP) led to the formation of the same product (see Figure 6) obtained using FPP as a substrate, thus demonstrating that **4b** is a *bona fide* substrate for the enzyme, although the rate of product formation was approximately 10-fold slower than with FPP. Based on these promising results, [$^{32}$P]**4b** was also examined for its ability to label the enzyme. Photolysis of NoSTSase with [$^{32}$P]**4b** resulted in labeling of the enzyme (See Figure 7, Lane 1) and significant protection was obtained when FPP was included in the photolysis reaction mixture (Figure 7, Lane 2) similar to that observed with the other enzymes reported here.

### 2.4. Modeling of 4b in the active sites of FPP-utilizing enzymes

In the design of **4a** and **4b**, a phosphonate was used to link the benzophenone unit to the farnesyl phosphate moiety. An important result of this is the removal of one oxygen atom relative to farnesyl diphosphate. Given that a number of interactions between the diphosphate group and residues from the protein typically occur in the active sites of FPP utilizing enzymes, it was decided to model **4b** in the active sites of three of the enzymes employed in this study. Since no crystal structure ScPFTase exists, the structure for RnPFTase (Rattus norvegicus) was used instead.[46] For that model the benzophenone phosphonate moiety was appended onto the farnesyl diphosphate group present in the active site of the binary (RnPFTase•FPP) complex and a conformational search was performed to identify to the lowest energy conformations. The structure surrounding the diphosphate of FPP from the RnPFTase•FPP complex is shown in Figure 8 (Top Left) with the corresponding region from the RnPFTase•**4b** complex (Top Right). Many of the interactions between the distal phosphate (from FPP) and the protein appear to be retained in the modeled structure of the RnPFTase•**4b** complex; that list includes interactions with K164α, H248β and Y300β. However, interactions with R291β and K294β are absent due to the absence of the one missing oxygen atom. A similar approach was used to create a model for EcFPP synthase.[47] The structure surrounding the diphosphate of FPP from the EcFPPSase•FPP complex is shown in Figure 8 (Middle Left) with the corresponding region from the EcFPPSase•**4b** complex (Middle Right). Residues that interact with the distal

phosphate (from FPP) and the phosphonate (from **4b**) include K66 R117 and K258; however, in the case of R117, it should be noted that due to the absence of one oxygen atom (due to the phosphonate substitution), one interaction between the terminal guanidino nitrogen is missing along with a longer range interaction with the internal guanidino nitrogen. Since no crystal structure of the NoSTSase employed here was available, the structure of a related enzyme, StSTSase (pentalenene synthase from Streptomyces Sp. UC5319)[48] was used; mutants of that enzyme produce germacrene.[49, 50] In this case, modeling was carried out using a docking algorithm. The structure surrounding the diphosphate of FPP from the StSTSase•FPP complex is shown in Figure 8 (Bottom Left) with the corresponding region from the StSTSase•**4b** complex (Bottom Right). In the case of StSTSase, most of the interactions between the diphosphate group and the enzyme are mediated by two $Mg^{2+}$ cations; all of these interactions are preserved in the StSTSase•**4b** model. However, several interactions between the distal phosphate and R173 are not present in the StSTSase•**4b** complex.

## 3. Discussion

To create a probe that would be capable of labeling residues in proximity to the diphosphate binding site of enzymes that employ FPP as a substrate, two photoactive molecules, **4a** and **4b**, were prepared in four (**4a**) or five steps (**4b**) from farnesyl monophosphate (**9**) and suitably functionalized phosphonate precursors. These compounds were competitive inhibitors of PFTase with respect to FPP with $IC_{50}$ values less than 6 μM.; analogue **4b** manifests a $K_I$ of 0.48 μM. In general, those values are comparable to those obtained earlier photoactive FPP analogues such as **2** and **3** (see Table 1) that incorporate the photophore into the isoprenoid moiety itself. Thus it appears that this new class of isoprenoid probes retain significant affinity for their cognate binding sites despite modification of one of the diphosphate oxygen atoms. Since the last step in the synthesis is the coupling of farnesyl monophosphate to a benzophenone phosphonate fragment, the preparation of radiolabeled forms of the probes can be easily accomplished from commercially available terpenoid precursors; accordingly, we prepared $^{32}$P-labeled forms of **4a** and **4b** and evaluated their ability to label PFTase. Both of these probes undergo crosslinking reactions with PFTase upon photolysis at 350 nm resulting in predominant labeling of the β-subunit of this heterodimeric enzyme; that labeling is abolished when photolysis is performed in the presence of the natural ligand, FPP. These results are consistent with the isoprenoid binding site being composed of residues primarily located on the β-subunit as evidenced from numerous x-ray crystal structures containing bound isoprenoid analogues.[10, 11, 37, 51, 52] Overall, these results demonstrate that **4a** and **4b** bind to an FPP-utilizing enzyme in a predictable fashion similar to results obtained with other photoprobes. Moreover, the absence of crosslinking to the α-subunit indicates that these probes manifest selectivity in their photoaffinity labeling reactions. Having established this, we then examined their interactions with several other types of enzymes that use FPP as a substrate or generate it as a product. FPPSases from *E. coli* and *D. melanogaster* are both labeled by **4b** upon photolysis. Since FPPSases from insect sources are involved in the biosynthesis of certain pheromones, these probes should be useful in functional studies of such proteins. Compound **4b** also labels a sesquiterpene synthase from *Nostoc sp. strain PCC7120* upon photolysis and interestingly, this probe is an alternative substrate for that enzyme. Given the large number of sesquiterpene synthases present in nature, these new probes should be highly useful for identifying sesquiterpene synthases from new sources. They may also be helpful in analyzing FPP binding to previously uncharacterized enzymes and for mapping their active sites. We are currently employing these molecules to assist in the identification of FPP-utilizing enzymes from a variety of sources. Finally, we note that molecular modeling of the complexes between various FPP-utilizing enzymes and **4b** suggests that these enzymes are able to interact with phosphonate present in **4b** in agreement with the studies reported here. However, the substitution of carbon in place of oxygen (compare the distal phosphate in FPP with the phosphonate in **4b**) does eliminate some specific interactions between the probe and the various

enzymes that results in decreased affinity. Significantly, despite their reduced affinity, **4a** and **4b** still bind with significant avidity. The $K_I$ using **4b** with ScPFTase (0.48 μM) is only 6-fold higher than the $K_D$ (0.075 μM) for FPP binding to ScPFTase. Interestingly, the decrease affinity for ScPFTase caused by the phosphonate substitution is comparable to that resulting from modest modification of the isoprenoid itself (see Table 1). These results suggest that phosphonate substitutions may be useful for the design of other probes designed to target FPP-utilizing enzymes.

## 4. Experimental

### 4.1. General

All reagents were obtained from Aldrich. Analytical TLC was performed on precoated (0.25 mm) silica gel 60F-254 plates purchased from E. Merck. Flash chromatography silica gel (60–120 mesh) was obtained from E. M. Science. HPLC analysis was carried out using a Beckman Model 127/166 instrument equipped with a diode array UV detector. Analytical separations employed a Rainin Dynamax-60 Å $C_{18}$ column (4.6 mm x 25 cm with a 2 cm guard column). GC/MS analysis was carried out on a Varian 3800 gas chromatograph linked to an ion-trap mass spectrometer employing a HP-1ms (Agilent Tech. Inc.) capillary column (30 m x 0.25 mm inner diameter, 1.5 μm film thickness) with He (g) as a carrier. Solid phase micro extraction (SPME) fibers (100 μm polydimethylsiloxane fiber) were obtained from Supelco. Phosphorimaging analysis was performed with a Molecular Dynamics 445 SI Phosphorimager. Dowex 50W–X8 resin was obtained from Bio-Rad and Sep-Pak columns were purchased from Waters. [$^{32}$P]$H_3PO_4$ (specific activity 8500–9120 Ci/mmol) was purchased from DuPont NEN. *N*-dansyl-GCVIA was synthesized by Dr. Dan Mullen in the Department of Chemistry, University of Minnesota. The enzymes used in this study were purified as previously described for yeast PFTase,[15] EcFPPSase,[43] DmFPPSase,[44] and NpSTSase.[45]

### 4.2 Chemical synthesis

**4.2.1. 3-bromo-methyl-benzophenone (6a)—**To a solution of 3-methyl-benzophenone (**5a**, 100 mg, 0.51 mmol) in CCl4 (7.0 mL) was added *N*-bromosuccinimide (NBS, 102 mg, 0.57 mmol) and azobisisobutyronitrile (AIBN, 0.52 mg, 0.02 mmol). The mixture was allowed to react at reflux for 24 h. The solvent was evaporated under vacuum and the crude material was used in the next reaction without purification. $^1$H NMR (300 MHz, $CDCl_3$) δ = 4.52 (s, 2H), 7.42–7.52 (m, 3H), 7.57–7.63 (m, 2H), 7.69–7.73 (ddd, 1H, J = 1.5, 1.5, 7.5 Hz) 7.78–7.84 (m, 3H). $^{13}$C NMR (75 MHz, $CDCl_3$ δ = 32.7, 128.5, 128.9, 130.1, 130.5, 132.7, 133.0, 137.3, 138.2, 138.3, 196.0. HRMS (ESI) (m/z): $[M+Na]^+$ calcd for $C_{14}H_{11}BrONa$ 296.9891 and 298.9870, found 296.9876 and 298.9861.

**4.2.2 (3-Benzoyl-benzyl)-phosphonic acid dimethyl ester (7a)—**A solution of crude 3-bromo-methyl-benzophenone (crude **6a**, estimated to be 0.51 mmol, prepared as described above) was dissolved in $P(OCH_3)_3$ (5.0 mL) and refluxed for 12 h. Excess trimethyl P $(OCH_3)_3$ was evaporated under vacuum and the resulting crude material was purified via silica gel chromatography (Hexanes/EtOAc, 1:1, v/v) to yield 131 mg (85% from **5a**). $^1$H NMR (300 MHz, $CDCl_3$) δ = 3.16 (d, 2H, J = 22 Hz), 3.62 (d, 6H, J = 11 Hz), 7.32–7.40 (m, 4H) 7.46–7.51 (m, 1H) 7.66–7.71 (m, 4H). $^{13}$C NMR (75 MHz, $CDCl_3$) δ = 32.6 (d, J = 138 Hz), 52.9 (d, J = 6.3 Hz), 128.3, 128.6 (d, J = 3.1 Hz), 128.7 (d. J = 3.7 Hz), 130.0, 131.2 (d, J = 6.8 Hz), 131.8 (d, J = 9.5 Hz), 132.5, 133.7 (d, J = 5.8 Hz), 137.4, 137.9 (d, J = 2.6 Hz), 196.2. $^{31}$P NMR (121 MHz, $CDCl_3$) δ = 28.9.

**4.2.3. (3-Benzoyl-benzyl)-phosphonic acid (8a)—**A solution of dimethyl ester **7a** (200 mg, 0.66 mmol) was refluxed in an aqueous solution of 4N HCl (7 mL) and dioxane (7 mL) over 12 h. The reaction mixture was extracted with EtOAc (20 mL, 4 times) and the resulting

product (89 mg, 49%) was deemed to be of sufficient purity to use in the next step without additional purification. $^{1}$H NMR (300 MHz, $CDCl_3$) δ = 3.02 (d, 2H, J = 21 Hz), 7.27–7.36 (m, 3H) 7.43–7.47 (m, 3H) 7.57 (s, 1H), 7.64 (d, 2H, J = 7.2 Hz). $^{13}$C NMR (75 MHz, $CDCl_3$) δ = 34.1 (d, J = 134 Hz), 128.2, 130.0, 131.2 (d, J = 6.3 Hz), 132.7, 133.4 (d, J = 9.0 Hz), 134.0 (d, J = 5.9 Hz), 137.1, 137.4, 197.4. $^{31}$P NMR (121 MHz, $CDCl_3$) δ = 24.9. HRMS (ESI) (m/z): [M-H]- calcd for $C_{14}H_{12}O_4P$ 275.0479, found 275.0461.

**4.2.4. 3-benzoylbenzylphosphonic ((2E,6E)-3,7,11-trimethyldodeca-2,6,10-trienyl phosphoric) anhydride (4a)—**Phosphonic acid **8a** (90 mg, 0.33 mmol) and CDI (79 mg, 0.39 mmol) were dissolved in DMF (1.5 mL) and allowed to react at room temperature under argon for 2 h, at which time farnesyl phosphate (**9**, cyclohexylamine salt) was added (130 mg, 0.326 mmol). The mixture was allowed to react for 7 days with stirring at room temperature. At that point, the reaction was quenched with water (5 mL) and extracted with EtOAc (10 mL, 4 times). The combined organic layers were dried over $Na_2SO_4$, filtered and concentrated to afford yellow oil. It was then dissolved in a solvent mixture composed of 50% $CH_3CN$ and 50% aqueous 25 mM $NH_4HCO_3$/isopropanol (50:1, v/v). This solution was applied to an ionic exchange column (Dowex 50×8–400, 2.6 × 4.5 cm), previously washed with aqueous $NH_4OH$ and equilibrated to pH 6.0 with aqueous 25 mM $NH_4HCO_3$/isopropanol (50:1, v/v). The column was eluted with additional aqueous 25 mM $NH_4HCO_3$/isopropanol (50:1, v/v) and the fractions containing the desired compound were concentrated by lyopholization. Final purification was accomplished via reversed-phase HPLC using 25 mM $NH_4HCO_3$ (solvent A) and $CH_3CN$ (solvent B) and the following elution profile performed at 5.0 mL/min: 5.0 min 0% solvent B; linear gradient from 0% to 60% solvent B over 40 min. Under these conditions the desired product eluted at 37 min. The solvent mixture was removed by lyopholization to afford 29 mg (15%) of a white solid. $^{1}$H NMR (500 MHz, $CDCl_3$) δ = 1.51 (s, 3H), 1.52 (s, 3H), 1.55 (s, 3H), 1.63 (s, 3H), 1.92–1.98 (m, 8H), 3.1 (d, 2H, J = 21.6 Hz), 4.22 (dd, 2H, J = 5.7 Hz), 5.01–5.03 (m, 2H), 5.22 (t, 1H, J = 6.5 Hz), 7.27–7.34 (m, 2H), 7.39–7.44 (m, 2H), 7.52–7.54 (m, 2H), 7.70–7.75 (m, 3H). $^{31}$P NMR (202 MHz, $CDCl_3$) δ = 11.5 (d, J = 23.1 Hz), −10.3 (d, J = 22.6 Hz). HRMS (ESI) (m/z): $[M-H]^-$ calcd for $C_{29}H_{37}O_7P_2$ 559.2020, found 559.2042. UV ε = 15.7 $mM^{-1}•cm^{-1}$ at 260 nm.

**4.2.5. (4-Benzoyl-benzyl)-phosphonic acid dimethyl ester (7b)—**The procedure employed here was identical to that used for the preparation of **7a**. Starting from 300 mg (1.1 mmol) of the bromide **6b**, 298 mg (90% yield) of the desired diester product **7b** was obtained. $^{1}$H NMR (300 MHz, $CDCl_3$) δ = 3.16 (d, 2H, J = 22 Hz), 3.62 (d, 6H, J = 11 Hz), 7.32–7.40 (m, 4H) 7.46–7.51 (m, 1H) 7.66–7.71 (m, 4H). $^{13}$C NMR (75 MHz, $CDCl_3$) δ = 32.9 (d, J = 137 Hz), 52.9 (d, J = 6.9 Hz), 128.3, 129.7 (d, J = 6.8 Hz), 129.9, 130.4 (d, J = 3.1 Hz), 132.4, 136.2 (d, J = 3.7 Hz), 136.4 (d, J = 9.5 Hz), 137.5, 196.1. $^{31}$P NMR (121 MHz, $CDCl_3$) δ = 28.2.

**4.2.6. (4-Benzoyl-benzyl)-phosphonic acid (8b)—**The procedure employed here was identical to that used for the preparation of **8a**. Starting from 200 mg (0.66 mmol) of the diester **7b**, 90 mg (49% yield) of the desired phosphonic acid product **8b** was obtained. $^{1}$H NMR (300 MHz, $CDCl_3$) δ = 3.24 (d, 2H, J = 22.2 Hz), 7.46–7.53 (m, 4H), 7.60–7.65 (m, 1H), 7.70–7.74 (m, 4H). $^{13}$C NMR (75 MHz, $CDCl_3$) δ = 34.9 (d, J = 134 Hz), 128.3, 129.7. 129.8, 129.9, 130.2, 130.2, 132.6, 135.7, 137.4, 138.2 197.2. $^{31}$P NMR (121 MHz, $CDCl_3$) δ =23.6. HRMS (ESI) (m/z): $[M-H]^-$ calcd for C14H12O4P 275.0479, found 275.0466.

**4.2.7. 4-benzoylbenzylphosphonic ((2E,6E)-3,7,11-trimethyldodeca-2,6,10-trienyl phosphoric) anhydride (4b)—**The procedure for the synthesis of **4b** was identical to that for **4a**. Starting from 90 mg (0.33 mmol) of the phosphonic acid **8b**, 33 mg (17% yield) of the desired product **4b** was obtained. The product eluted at 36 min (HPLC with same

conditions than **4a**). $^{1}$H NMR (300 MHz, $CDCl_3$) δ = 1.34 (s, 3H), 1.35 (s, 3H), 1.39 (s, 3H), 1.43 (s, 3H), 1.71–1.82 (m, 8H), 3.0 (d, 2H, J = 22.2 Hz), 4.11 (dd, 2H, J = 6.3 Hz), 4.83–4.84 (m, 2H), 5.11 (t, 1H, J = 6.6 Hz), 7.23–7.28 (m, 4H), 7.35–7.38 (m, 1H), 7.47–7.53 (m, 4H). $^{31}$P NMR (121 MHz, $CDCl_3$) δ =-9.6 (d, J = 25.3 Hz), 12.1 (d, J = 25.9 Hz). HRMS (ESI) (m/z): $[M-H]^-$ calcd for C29H37O7P2 559.2020, found 559.2076. UV δ = 17.8 $mM^{-1}•cm^{-1}$ at 272 nm

**4.2.8. [$^{32}$P]-4-benzoylbenzylphosphonic ((2E,6E)-3,7,11-trimethyldodeca-2,6,10-trienyl phosphoric) anhydride ([$^{32}$P]4b)—**The synthesis of [$^{32}$P]**4b** accomplished in two steps. First, [$^{32}$P]-labeled farnesyl monophosphate was prepared via phosphorylation of farnesol using a procedure similar to that we have previously employed for the preparation of isoprenyl diphosphates. Carrier free [$^{32}$P]-$H_3PO_4$ (5 mCi) was diluted with unlabeled $H_3PO_4$ (1.6 mg, 20 μmol) and lyophilized. To the resulting anhydrous $H_3PO_4$ was added a solution of triethylamine (4.1 mg, 40 μmol) in $CH_3CN$ (50 μL). Farnesol (4.4 mg, 20 μmol) in 200 μL of $CH_3CN$ containing 20% of $CCl_3CN$ (v/v) was then added and the reaction was allowed to stir under N2 for 2 h after which time the volatile components were removed under a stream of $N_2$. The crude material was purified with a Sep-Pac reversed phase $C_{18}$ column using a stepwise gradient of $CH_3CN$ and 25 mM $NH_4HCO_3$ and the fractions containing [$^{32}$P]**9** (determined by TLC: i-PrOH/$NH_4OH$/$H_2O$, 6:3:1 v/v/v, $R_f$ = 0.62, visualized by phosphoroimaging analysis) were pooled and lyophilized under vacuum. The benzophenone phosphonic acid derivative (**8b**, 5.5 mg, 20 μmol) was dissolved in anhydrous DMF (400μL), under Ar (g) at room temperature. CDI (3.9 mg, 24 μmol) was added and the resulting activation reaction was left stirring 2 h before it was added to the lyophilized [$^{32}$P]**9**. The reaction was allowed to react for 2 days at which time the DMF was removed under a stream of $N_2$ (g). The crude material was purified with a Sep-Pak reversed phase $C_{18}$ column using a stepwise gradient of $CH_3CN$ and 25 mM $NH_4HCO_3$. The product eluted at 30% of $CH_3CN$ (specific activity 197 Ci/mol). The radiochemical purity was assessed by TLC (i-PrOH/$NH_4OH$/$H_2O$, 6:3:1 v/v/v, $R_f$ = 0.7, 81% of product) followed by phosphoroimaging analysis.

### 4.3. Biological Experiments

**4.3.1. Farnesyltransferase Assays—**$IC_{50}$ values were determined for **4a** and **4b** with ScPFTase by running duplicate assays with FPP and *N*-Ds-GCVIA maintained at 2.4 μM and **4a** or **4b** at concentrations of 0, 1, 2, 3, 5, 10 and 20 (μM. An enzyme concentration of 5.0 nM ScPFTase was employed. $IC_{50}$ values were calculated from a direct fit of the rate versus inhibitor concentration data using KaleidaGraph software. Based on those results, a more systematic study was performed with **4b** using a 4 × 6 grid of duplicate assays with FPP maintained at fixed concentrations (1, 2, 5, and 7.0 μM) and varying concentrations of **4b** (0, 0.2, 0.4, 0.7, 1, 1.5 and 2 (μM for **4b**). In those experiments, the concentration of ScPFTase was 5 nM, and the concentration of *N*-Ds-GCVIA was fixed at 2.4 (μM. The rates were determined from the initial velocity measurements and $K_I$ value calculated from an Eadie-Hofstee plot.[41, 42]

**4.3.2. Photolabeling Reactions—**All photolysis reactions were conducted at 4 °C in a UV Rayonet mini-reactor equipped with six RPR-3500 Å lamps and a circulating platform that allows up to eight samples to be irradiated simultaneously. All reactions (100 μL) were performed in silinized quartz test tubes (10 × 75 mm) and contained 52 mM Tris•HCl, pH 7.0, 5.8 mM DTT, 12 mM $MgCl_2$, 12 (μM $ZnCl_2$, 25 mM NH4HCO3 and the targeted enzyme at 50 μg/mL. Where appropriate, reactions contained [$^{32}$P]**4a** (29 μM) or [$^{32}$P]**4b** (29 μM); these concentrations were chosen to be 10 times above their experimentally measured $K_I$ values (for ScPFTase). For substrate protection experiments, FPP was added to a final concentration of 100 μM. Reactions were photolyzed for 6 h using the apparatus described above. Loading buffer [50 μL; 4.0% SDS, 12% glycerol (w/v), 50 mM Tris•HCl, 2.0% 2-mercaptoethanol (v/

v), 0.01% bromophenol blue] was then added to each sample, and the samples were heated to 70°C for 20 min followed by analysis by SDS-polyacrylamide gel electrophoresis using a 12% Tris-Tricine gel. Gels were first stained with Comassie Blue or Sypro Orange to visualize the proteins followed by phosphorimaging analysis to assess the extent of crosslinking that was subsequently quantified via volume integration of the labeled protein bands (after subtraction of any background signal).

#### 4.3.3. In Vitro Reactions with the Germacrene Producing Cyclase (NoSTSase)—

Reactions were performed by incubating 10 μg of purified enzyme[45] in 200 μL of reaction buffer (10 mM $MgCl_2$ and 1.0 mM 2-mercaptoethanol in 10 mM Tris•HCl, pH 8.0) with varying concentrations of probe **4b** or FPP (50, 100 or 200 μM) in a sealed glass vial. After reaction for 18 h at 25 °C, the headspace gas was sampled for 10 min by SPME using a 100 μm polydimethylsiloxane fiber. Afterwards, the full fiber was inserted into the injection port of a GC/MS for analysis. Compounds bound to SPME fibers were desorbed for 20 min in the injection port (250 °C) followed by gas chromatographic separation using a temperature program that ramped from 60 °C to 250 °C at a rate of 20 °C/min. Mass spectra were scanned in the range of 5–300 atomic mass units at 1 s intervals.

### 4.4. Modeling of 4b in the active sites of FPP-utilizing enzymes

For modeling of the RnPFTase•**4b** complex, the benzophenone moiety in **4b** was built by modifying the existing FPP present in the crystal structure of the enzyme (1JCR).[46] Once modified, a 5000 step mixed torsional/low-mode conformational search was conducted with MacroModel (Schrodinger, version 9.6) using the OPLS forcefield.[53, 54] The rotatable bonds in the flexible tail of the ligand were specifically chosen for torsional sampling, and the protein was frozen throughout the search. The resulting conformation with the lowest potential energy was chosen for display. For EcFPPSase, FPP and the **4b** were built by modifying the existing IPP present in the crystal structure of the enzyme (1RQI).[47] A conformational search was performed as described for RnPFTase and the resulting conformation with the lowest potential energy was chosen for display of each ligand. For StSTSase (Pentalenene synthase),[55] FPP and **4b** were docked in the active site of the crystal structure of the enzyme (1PS1) using Glide (Schrodinger, version 5.0). A standard precision docking parameter was set and 10000 ligand poses per doking were run. The resulting conformation with the lowest docking score was chosen for display for each ligand.

## Supplementary Material

Refer to Web version on PubMed Central for supplementary material.

## Acknowledgments

This research was supported by the National Institutes of Health Grant GM58442 (M.D.D.), the National Science Foundation Grant DBI 0321690 (D. S.) and funds from Yulex Corp.

## References

1. Cane DE. Comp. Nat. Prod. Chem 1999;2:155.
2. Davis EM, Croteau R. Topics Curr. Chem 2000;209:53.
3. Loomis WD, Croteau R. Biochem. Plants 1980;4:363.
4. Cornish K. ACS Symp. Series 1992;497:18.
5. Zhang FL, Casey PJ. Ann. Rev. Biochem 1996;65:241. [PubMed: 8811180]
6. Fraga BM. Nat. Prod. Rep 2008;25:1180. [PubMed: 19030608]
7. Marecak DM, Horiuchi Y, Arai H, Shimonaga M, Maki Y, Koyama T, Ogura K, Prestwich GD. Bioorg. Med. Chem. Lett 1997;7:1973.

8. Zhang Y-W, Koyama T, Marecak DM, Prestwich GD, Maki Y, Ogura K. Biochemistry 1998;37:13411. [PubMed: 9748348]
9. Tian R, Li L, Tang W, Liu H, Ye M, Zhao ZK, Zou H. Proteomics 2008;8:3094. [PubMed: 18615431]
10. DeGraw AJ, Zhao Z, Hsieh J, Jefferies M, Distefano MD, Strickland CL, Shintani D, Nural H, McMahan C, Xie W. J. Org. Chem 2007;72:4587. [PubMed: 17477573]
11. Turek TC, Gaon I, Distefano MD, Strickland CL. J. Org. Chem 2001;66:3253. [PubMed: 11348105]
12. Kale TA, Raab C, Yu N, Dean DC, Distefano MD. J. Am. Chem. Soc 2001;123:4373. [PubMed: 11457220]
13. Turek TC, Gaon I, Gamache D, Distefano MD. Bioorg. Med. Chem. Lett 1997;7:2125.
14. Turek TC, Gaon I, Distefano MD. Tet. Lett 1996;37:4845.
15. Gaon I, Turek TC, Weller VA, Edelstein RL, Singh SK, Distefano MD. J. Org. Chem 1996;61:7738. [PubMed: 11667728]
16. Gaon I, Turek TC, Distefano MD. Tet. Lett 1996;37:8833.
17. Edelstein RL, Distefano MD. Biochem. Biophys. Res. Comm 1997;235:377. [PubMed: 9199201]
18. Allen CM, Baba T. Meth. Enzymol 1985;110:117. [PubMed: 4021809]
19. Baba T, Allen CM. Biochemistry 1984;23:1312.
20. Baba T, Muth J, Allen CM. J. Biol. Chem 1985;260:10467. [PubMed: 3897217]
21. Omer CA, Kral AM, Diehl RE, Prendergast GC, Powers S, Allen CM, Gibbs JB, Kohl NE. Biochemistry 1993;32:5167. [PubMed: 8494894]
22. Das NP, Allen CM. Biochem. Biophys. Res. Comm 1991;181:729. [PubMed: 1755854]
23. Yokoyama K, McGeady P, Gelb MH. Biochemistry 1995;34:1344. [PubMed: 7827082]
24. Rilling HC. Meth. Enzmol 1985;110:125.
25. Chehade KAH, Kiegiel K, Isaacs RJ, Pickett JS, Bowers KE, Fierke CA, Andres DA, Spielmann HP. J. Am. Chem. Soc 2002;124:8206. [PubMed: 12105898]
26. Turek TC, Gaon I, Distefano MD. J. Lab. Cmpds. Radiopharm 1997;39:140.
27. Turek, TC.; Edelstein, RL.; Gaon, I.; Weller, VA.; Distefano, MDIn. [32P]-labeled analogs of farnesyl and geranylgeranyl pyrophosphate: Synthesis and application in photoaffinity labeling experiments with protein prenyltransferases. Hays, JR.; Melilo, DG., editors. John Wiley & Sons Ltd; 1998. p. 67Synth. Appl. Isot. Labelled Compd. 1997, Proc. Int. Symp., 6th, 1998
28. Mayer MP, Prestwich GD, Dolence JM, Bond PD, Wu H-y, Poulter CD. Gene 1993;132:41. [PubMed: 8406041]
29. Dolence JM, Poulter CD. Proc. Nat. Acad. Sci. USA 1995;92:5008. [PubMed: 7761439]
30. Dolence JM, Cassidy PB, Mathis JR, Poulter CD. Biochemistry 1995;34:16687. [PubMed: 8527442]
31. Mathis JR, Poulter CD. Biochemistry 1997;36:6367. [PubMed: 9174352]
32. Rozema DB, Poulter CD. Biochemistry 1999;38:13138. [PubMed: 10529185]
33. Gibbs RA, Krishnan U, Dolence JM, Poulter CD. J. Org. Chem 1995;60:7821.
34. Zahn TJ, Eilers M, Guo Z, Ksebati MB, Simon M, Scholten JD, Smith SO, Gibbs RA. J. Am. Chem. Soc 2000;122:7153.
35. Reigard SA, Zahn TJ, Haworth KB, Hicks KA, Fierke CA, Gibbs RA. Biochemistry 2005;44:11214. [PubMed: 16101305]
36. Gibbs RA, Zahn TJ, Sebolt-Leopold JS. Curr. Med. Chem 2001;8:1437. [PubMed: 11562276]
37. Turek-Etienne TC, Strickland CL, Distefano MD. Biochemistry 2003;42:3716. [PubMed: 12667062]
38. Kale TA, Hsieh S-aJ, Rose MW, Distefano MD. Curr. Topics Med. Chem 2003;3:1043.
39. Pompliano DL, Gomez RP, Anthony NJ. J. Am. Chem. Soc 1992;114:7945.
40. Bond PD, Dolence JM, Poulter CD. Meth. Enzymol 1995;250:30. [PubMed: 7651159]
41. Hofstee BHJ. Science 1952;116:329. [PubMed: 12984118]
42. Eadie GS. J. Biol. Chem 1942;146:85.
43. Lee PC, Petri R, Mijts BN, Watts KT, Schmidt-Dannert C. Metab. Eng 2005;7:18. [PubMed: 15721807]
44. Sen SE, Trobaugh C, Beliveau C, Richard T, Cusson M. Insect Biochem. Mol. Biol 2007;37:1198. [PubMed: 17916506]

45. Agger SA, Lopez-Gallego F, Hoye TR, Schmidt-Dannert C. J. Bacteriol 2008;190:6084. [PubMed: 18658271]
46. Long SB, Hancock PJ, Kral AM, Hellinga HW, Beese LS. Proc. Nat. Acad. Sci. USA 2001;98:12948. [PubMed: 11687658]
47. Hosfield DJ, Zhang Y, Dougan Douglas R, Broun A, Tari Leslie W, Swanson Ronald V, Finn J. J Biol Chem 2004;279:8526. [PubMed: 14672944]
48. Cane DE, Sohng J-K, Lamberson CR, Rudnicki SM, Wu Z, Lloyd MD, Oliver JS, Hubbard BR. Biochemistry 1994;33:5846. [PubMed: 8180213]
49. Seemann M, Zhai G, de Kraker J-W, Paschall CM, Christianson DW, Cane DE. J. Am. Chem. Soc 2002;124:7681. [PubMed: 12083921]
50. Seemann M, Zhai G, Umezawa K, Cane D. J. Am. Chem. Soc 1999;121:591.
51. Park H-W, Boduluri SR, Moomaw JF, Casey PJ, Beese LS. Science 1997;275:1800. [PubMed: 9065406]
52. Strickland CL, Windsor WT, Syto R, Wang L, Bond R, Wu Z, Schwartz J, Le HV, Beese LS, Weber PC. Biochemistry 1998;37:16601. [PubMed: 9843427]
53. Jorgensen WL, Tirado-Rives J. J. Am. Chem. Soc 1988;110:1657.
54. Kaminski GA, Friesner RA, Tirado-Rives J, Jorgensen WL. J. Phys. Chem. B 2001;105:6474.
55. Lesburg CA, Zhai G, Cane DE, Christianson DW. Science 1997;277:1820. [PubMed: 9295272]

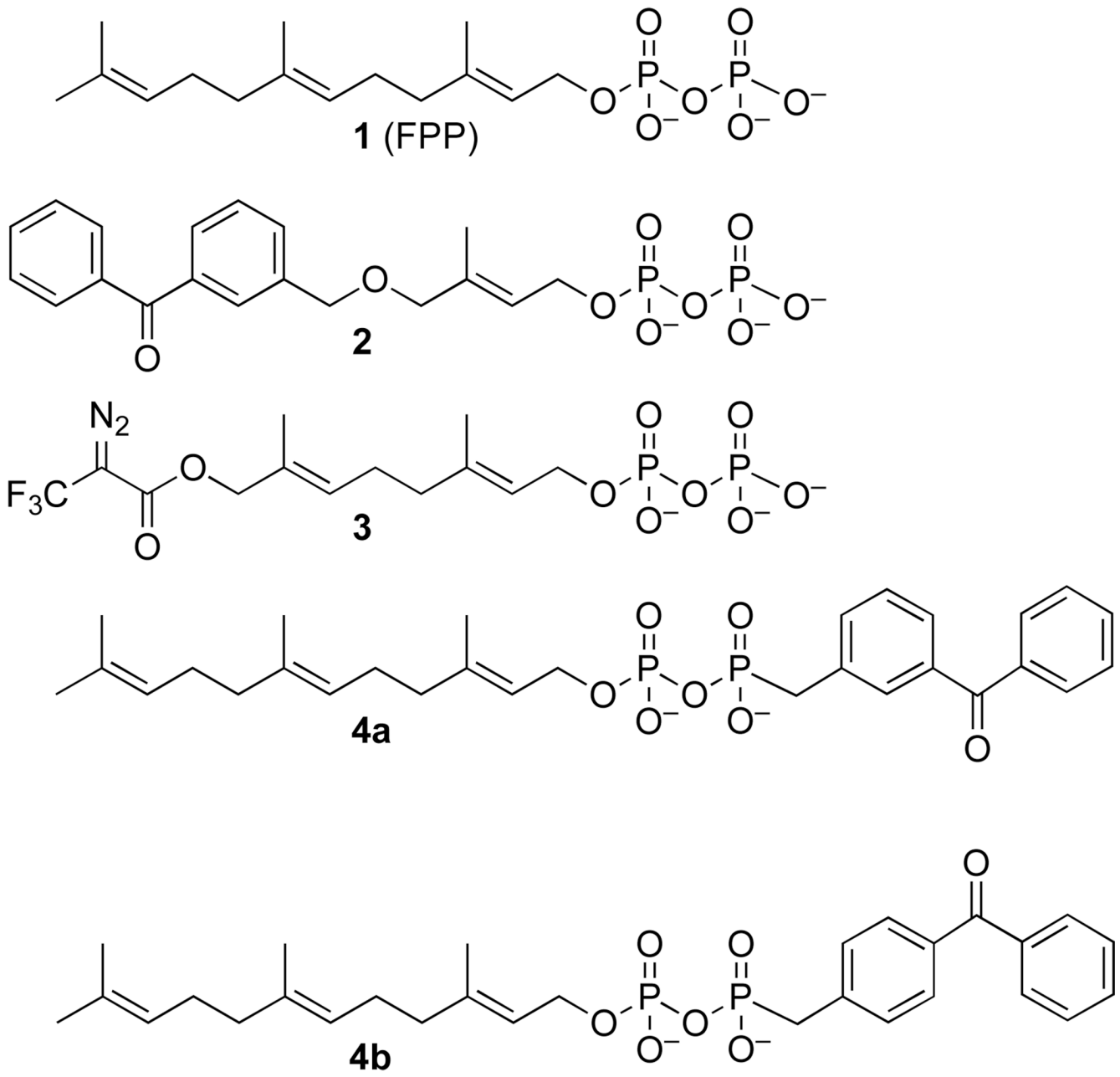


**Figure 1.**
Farnesyl diphosphate (FPP) and photoactive analogues

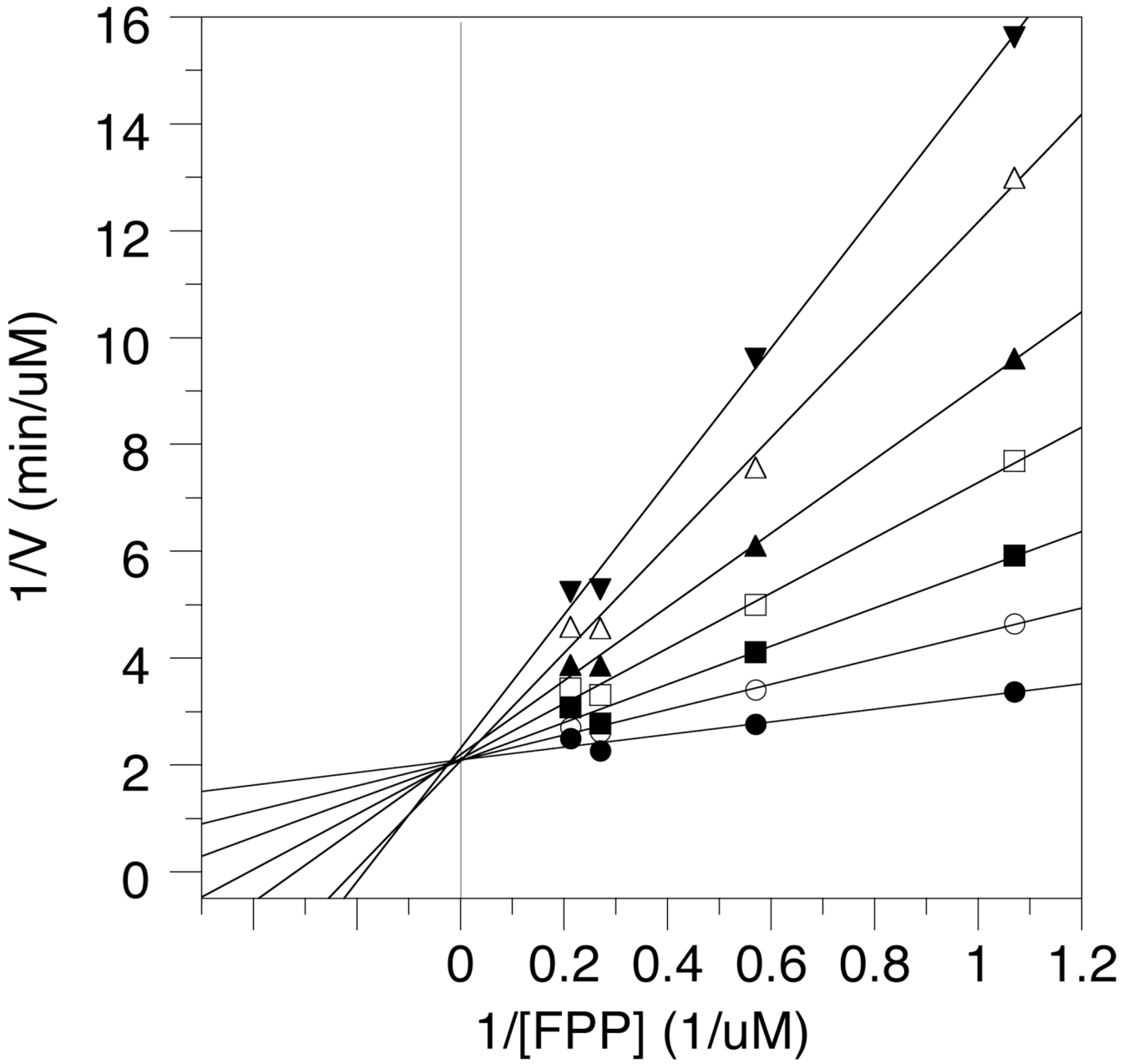


**Figure 2.**
Double reciprocal plot showing the competitive inhibition of ScPFTase by **4b**. The concentrations of **4b** used were as follows: (unknownsymbol28) 0 $\mu$M, (O) 0.2 $\mu$M, (▪) 0.4 $\mu$M, (□) 0.7 $\mu$M, (▲) 1.0 $\mu$M, (Δ) 1.5 $\mu$M, (▼) 2.0 $\mu$M.

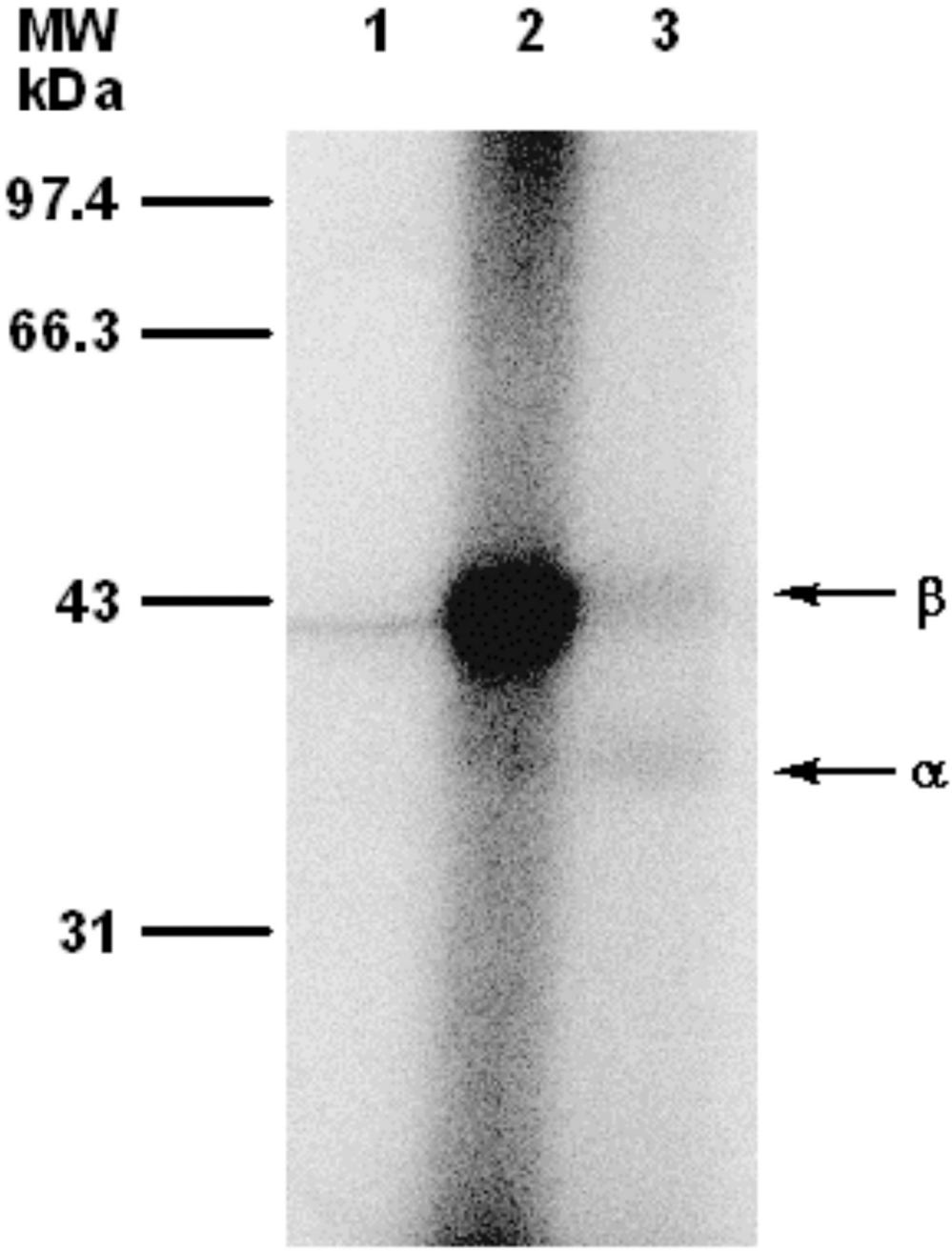


**Figure 3.**
Phosphorimaging analysis of photolabeling of ScPFTase with [$^{32}$P]**4b** after SDS-PAGE fractionation. Lane 1: ScPFTase and [$^{32}$P]**4b** (29 $\mu$M), no UV irradiation. Lane 2: ScPFTase and [$^{32}$P]**4b** (29 $\mu$M), with UV irradiation. Lane 3: PFTase, [$^{32}$P]**4b** (29 $\mu$M), and FPP (100 $\mu$M), with UV irradiation.

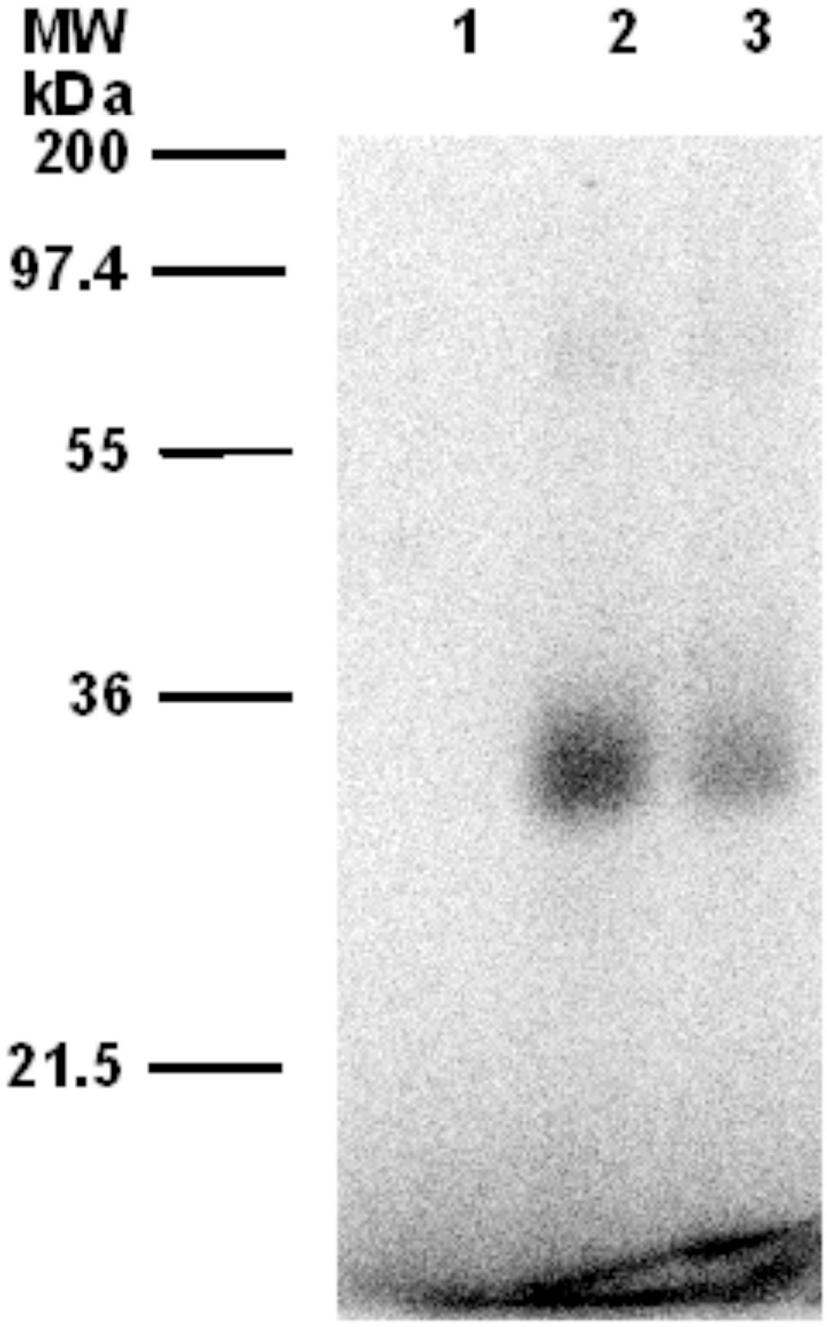


**Figure 4.**
Phosphorimaging analysis of photolabeling of EcFPPSase with [$^{32}$P]**4b** after SDS-PAGE separation. Lane 1: EcFPPSase and [$^{32}$P]**4b** (29 $\mu$M), no UV irradiation. Lane 2: EcFPPSase and [$^{32}$P]**4b** (29 $\mu$M), with UV irradiation. Lane 3: EcFPPSase, [$^{32}$P]**4b** (29 $\mu$M), and FPP (100 $\mu$M), with UV irradiation.

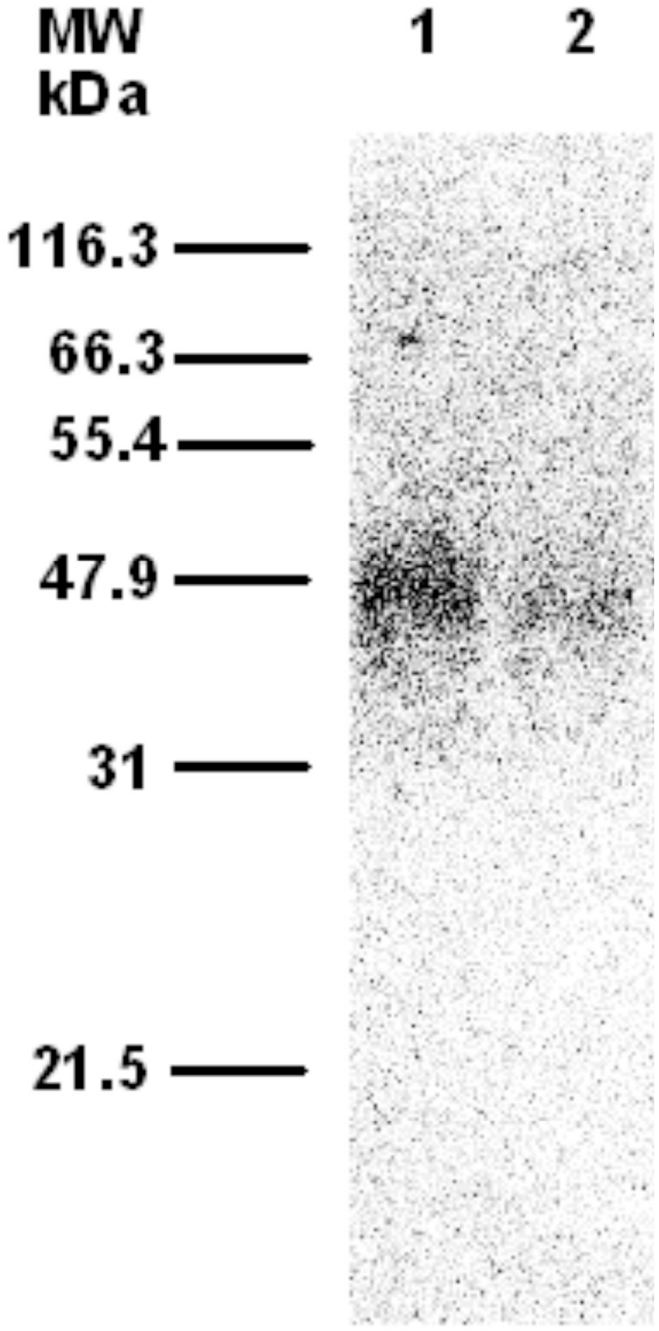


**Figure 5.**
Phosphorimaging analysis of photolabeling of DmFPPSase with [$^{32}$P]**4b** after SDS-PAGE separation. Lane 1: DmFPPSase and [$^{32}$P]**4b** (29 $\mu$M), with UV irradiation. Lane 2: DmFPPSase, [$^{32}$P]**4b** (29 $\mu$M), and FPP (100 $\mu$M), with UV irradiation.

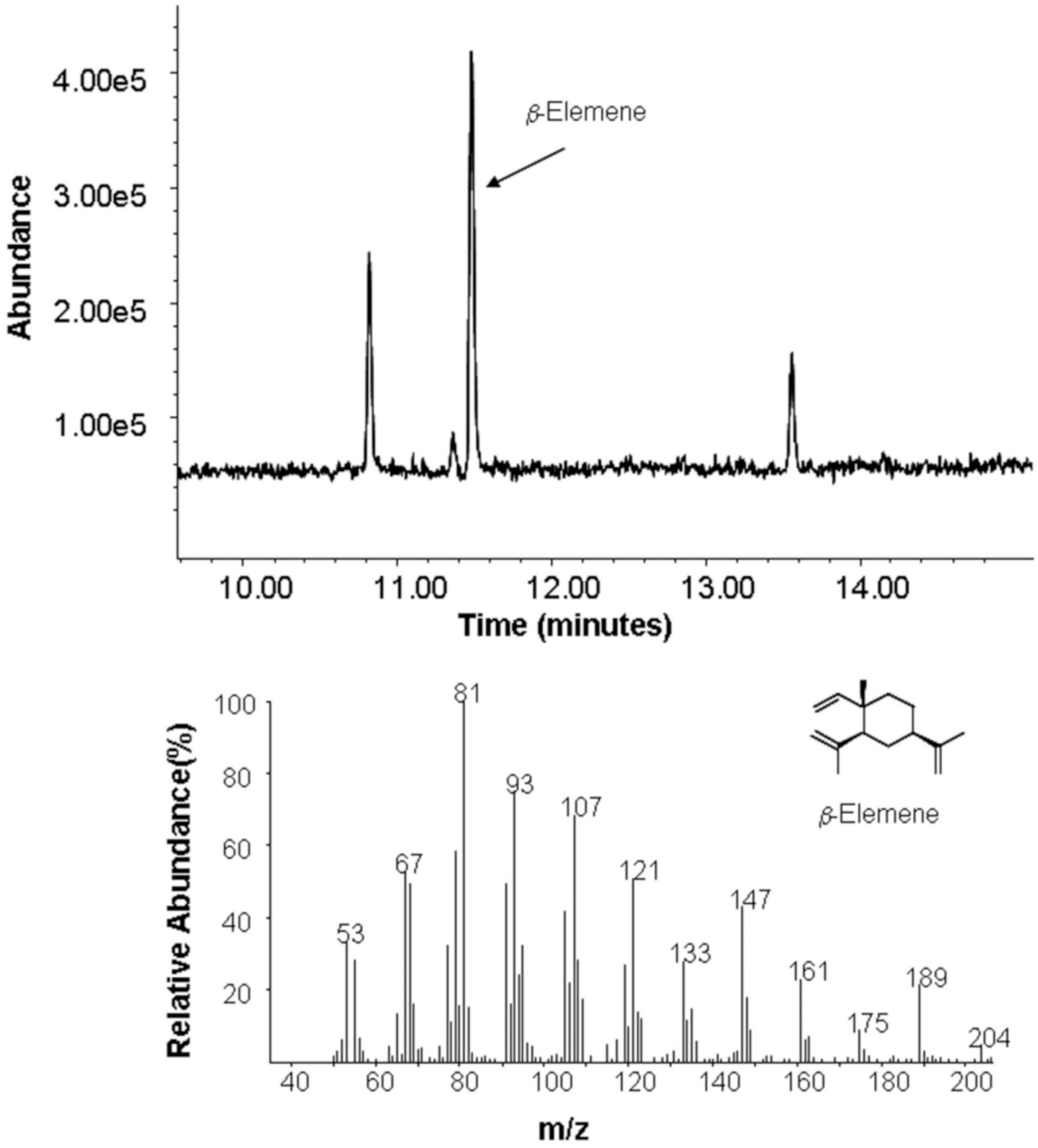


**Figure 6.**

Analysis of the product formed from incubation of **4b** with NoSTSase. Above: Gas chromatographic analysis of reaction. Below: MS the of product peak (Retention Time = 11.5 min). Note: It has been previously established that the product of the cyclization reaction (germacrene A) undergoes thermal rearrangement to β-elemene at the temperature of the GC injection port.[45]

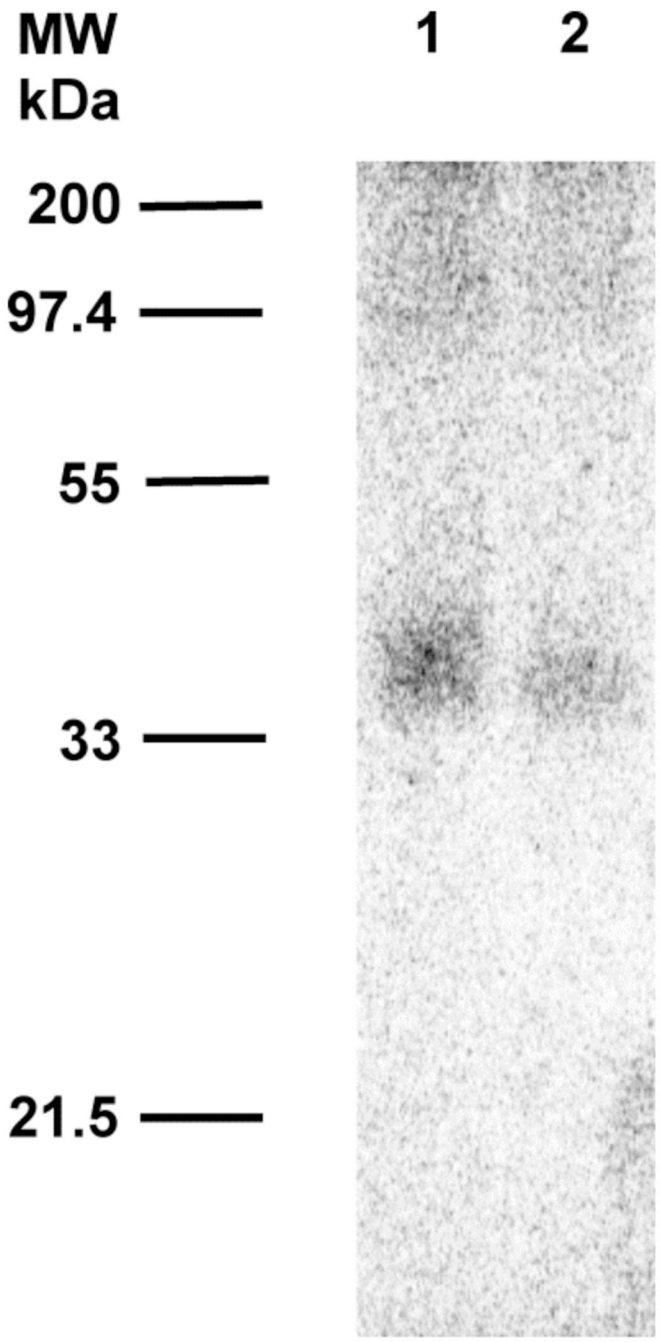


**Figure 7.**
Phosphorimaging analysis of photolabeling of NoSTSase with [$^{32}$P]**4b** after SDS-PAGE separation. Lane 1: NoSTSase and [$^{32}$P]**4b** (29 $\mu$M), with UV irradiation. Lane 2: NoSTSase, [$^{32}$P]**4b** (29 $\mu$M), and FPP (100 $\mu$M), with UV irradiation.

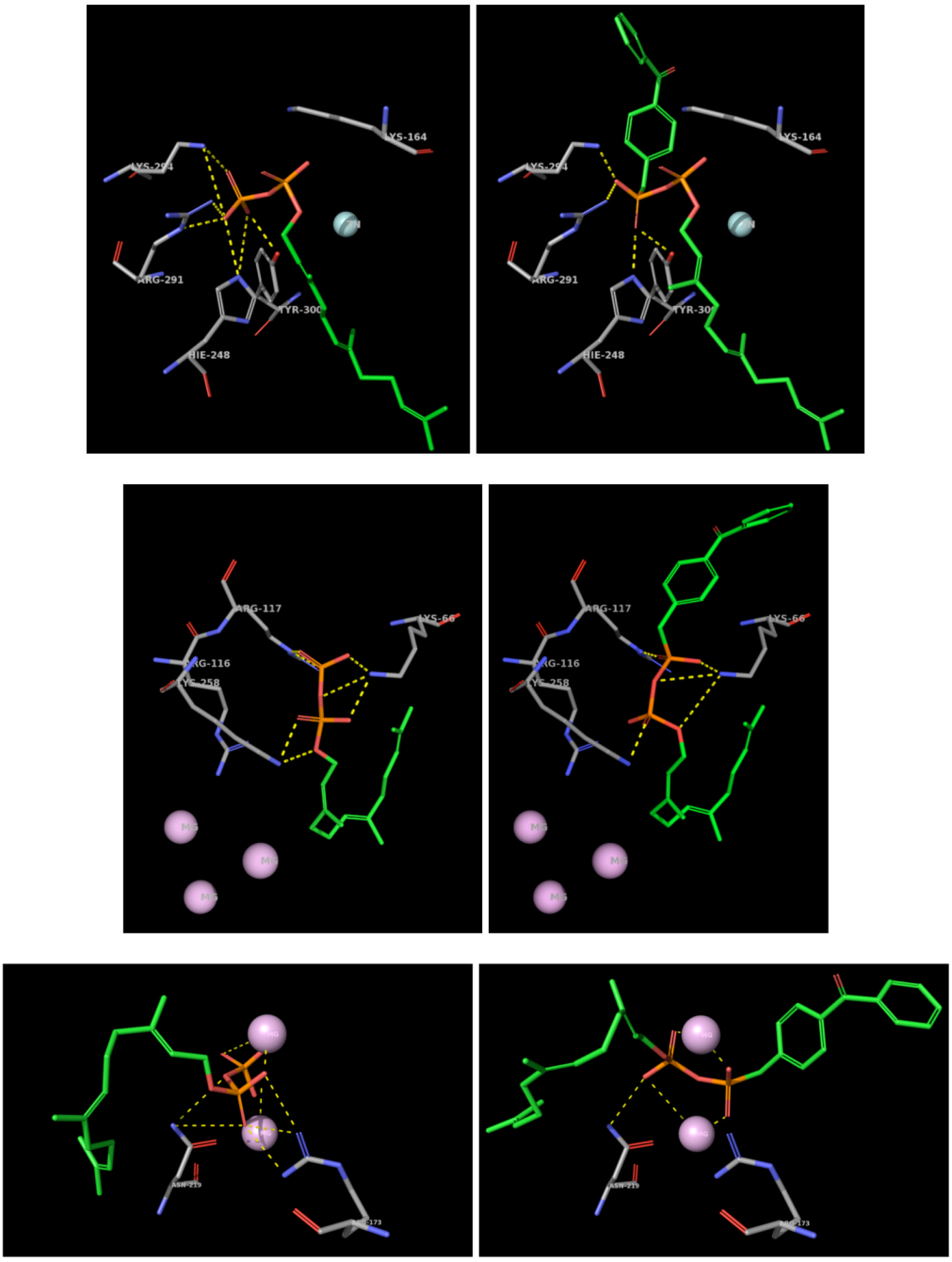


**Figure 8.**

Modeling of **4b** in the active sites of FPP-utilizing enzymes. Top Left: Crystal structure of NrPFTase (1JCR) with bound FPP. Shown, are residues H248β, R291β, K294β, Y300β, K164α (colored by element; carbon in grey), FPP (colored by element; carbon in green) and Zn (cyan). The yellow dashes illustrate potential hydrogen bonding or electrostatic interactions (within 4Å) of the distal phosphate. Top Right: Crystal structure of NrPFTase with **4b** built on the bound FPP. The color scheme is the same as that for Top Left. Middle Left: Crystal structure of EcFPPSase (1RQ1) with FPP built by modifying the existing bound IPP. Shown, are residues K66, R116, R117, K258 (colored by element; carbon in grey), FPP (colored by element; carbon in green) and Mg (purple). The yellow dashes illustrate potential hydrogen bonding or

electrostatic interactions (within 4Å) of the distal phosphate. Middle Right: Crystal structure of EcFPPSase with **4b** built on the bound IPP. The color scheme is the same as that for Middle Left. Bottom Left: Crystal structure of StSTSase (Pentalenene synthase, 1PS1) with FPP docked in the active site of the enzyme. Shown, are residues R173, N219 (colored by element; carbon in grey), FPP (colored by element; carbon in green) and Mg (purple). The yellow dashes illustrate potential hydrogen bonding or electrostatic interactions (within 4Å) of the distal phosphate. Bottom Right: Crystal structure of StSTSase with **4b** docked in the active site of the enzyme. The color scheme is the same as that for Bottom Left.

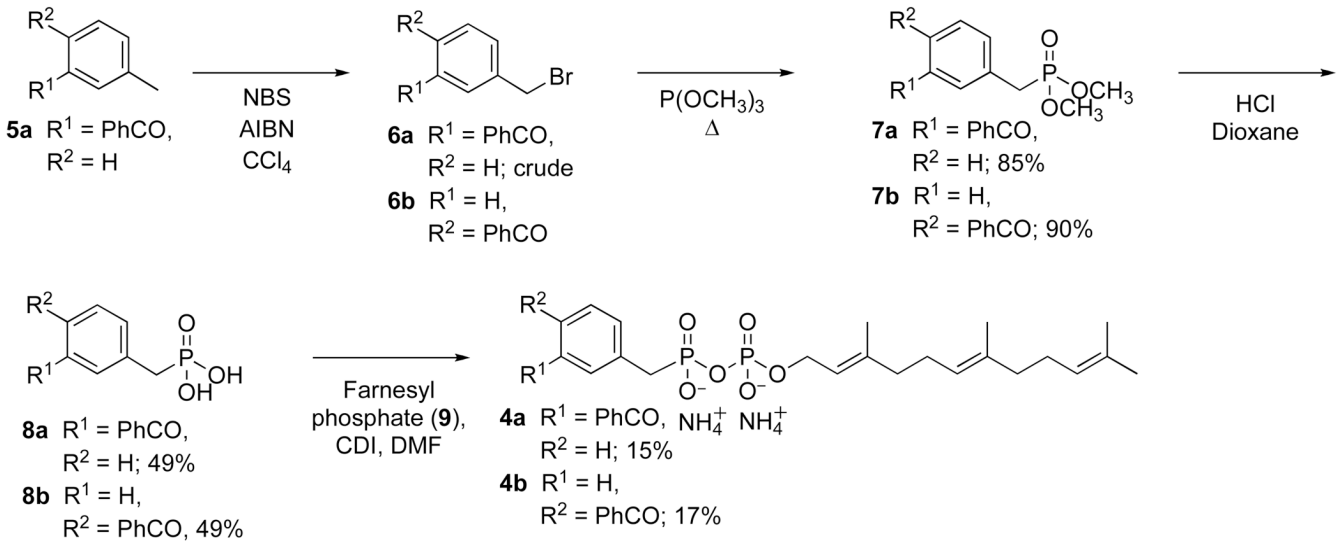


**Scheme 1.**
Synthesis of photoaffinity analogs **4a** and **4b**

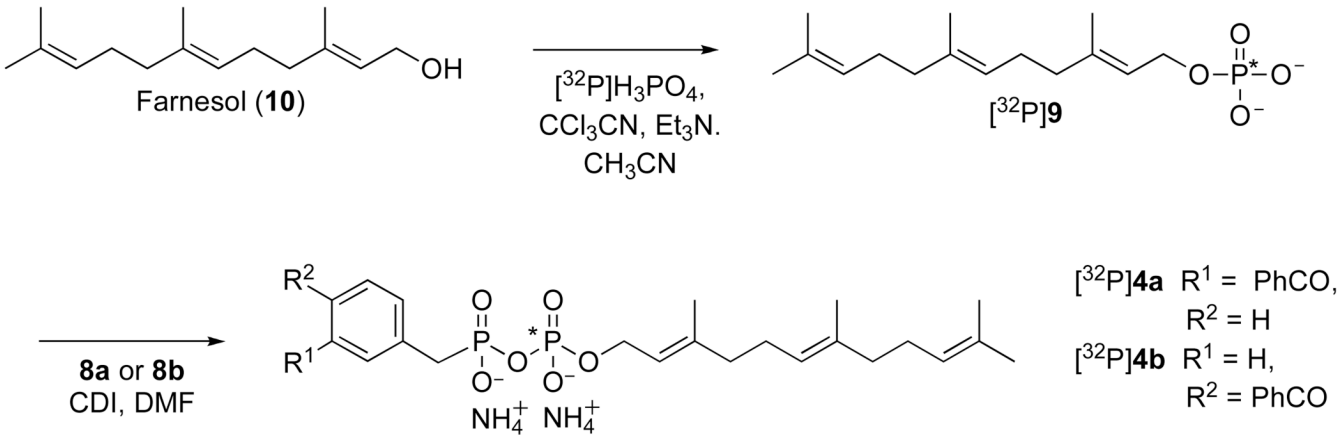


**Scheme 2.**
Synthesis of $^{32}$P-labeled forms of **4a** and **4b**. The position of the $^{32}$P radiolabel is indicated with a (*).

## Table 1

$IC_{50}$ and $K_I$ values for inhibition of PFTase with photoactive FPP analogues.

| Compound | $IC_{50}$ (μM) | $K_I$ (μM) |
|---|---|---|
| **1** (FPP) | - | 0.075[1] |
| **2**[2] | 3.4 | 0.61 |
| **3**[3] | 0.72 | 0.20 |
| **4a** | 5.8 | N.D.[4] |
| **4b** | 3.0 | 0.48 |

[1] From Dolence et al.[30]

[2] From Turek et al.[11]

[3] From Edelstein and Distefano.[17]

[4] Not Determined.